Picosecond mid-infrared optical parametric amplifier based on the wide-bandgap $GaS_{0.4}Se_{0.6}$ pumped by a Nd:YAG laser system at 1064 nm

Kentaro Miyata,[1,2] Georgi Marchev,[1] Aleksey Tyazhev,[1] Vladimir Panyutin,[1] and Valentin Petrov[1,*]

[1]*Max-Born-Institute for Nonlinear Optics and Ultrafast Spectroscopy, 2A Max-Born-Strasse, D-12489 Berlin, Germany*

[2]*MegaOpto, Co. Ltd., RIKEN Cooperation Center W414, 2-1 Hirosawa, Wako, Saitama 351-0198, Japan*

**Corresponding author: petrov@mbi-berlin.de*

Received February 7, 2011; revised March 16, 2011; accepted March 31, 2011;
posted April 11, 2011 (Doc. ID 142331); published May 10, 2011

Operation of a $GaS_{0.4}Se_{0.6}$ optical parametric amplifier is demonstrated with a 5–11 μm idler tuning range, maximum energies of ~10 μJ for sub-30-ps pulse durations, and performance ~3 times better than with pure GaSe.

OCIS codes: 190.4970, 190.4400.

Nonlinear optical crystals with composition GaS_xSe_{1-x}, $x = 0.2$ and 0.4, were studied as early as 1982 [1]. Relative measurements of the second-harmonic generation (SHG) conversion efficiency with a Q-switched CO_2 laser indicated substantial reduction of the nonlinear coefficient with the S content, $d_{22}(x = 0.2) = (0.525 \pm 0.05)d_{22}(\mathrm{GaSe})$ and $d_{22}(x=0.4)=(0.31\pm0.05)d_{22}(\mathrm{GaSe})$, which obviously contributed to the lack of interest in further investigation of such solid solutions.

According to [1], a phase transition from the noncentrosymmetric (ε) phase of GaSe, corresponding to the $\bar{6}m2$ point group, to a centrosymmetric (β) phase, corresponding to the $6/mmm$ point group, takes place for $0.2 < x < 0.3$. In [2], the limits of the possible polytypes occurring in the GaS_xSe_{1-x} solid solutions were given as ε for $x = 0$ (GaSe) to $x \sim 0.01$, ε–γ mixture for x between ~0.01 and ~0.03, γ for x between ~0.05 and ~0.4, and β for x from ~0.5 to 1 (GaS). Here, the γ phase corresponds to the noncentrosymmetric point group $3m$. More recent studies associated the mixed ε–γ phase with $0 \le x \le 0.4$, a mixture of ε–γ and β was observed for $x = 0.5$ and pure β phase for GaS [3]; see [4] for an overview. Nevertheless, the question about the transitions between the phases is very complex and has not yet found a satisfactory solution. Four phases were identified for GaSe itself in the literature, while GaS crystallizes only in the β phase. The literature on GaS_xSe_{1-x} compounds is often controversial concerning this issue and it seems that there is some dependence on the growth conditions [5,6].

The first phase-matched nonlinear frequency conversion process realized with GaS_xSe_{1-x} crystals was difference-frequency generation from 7 to 12.5 μm using $GaS_{0.2}Se_{0.8}$ [1]. More recently, the phase-matching properties of a series of solid solutions with x ranging from 0.04 to 0.412 were measured for SHG of 2.79 μm (Er:YSGG laser) and 9.56/9.58 μm (CO_2 laser) radiation [7,8]. Our estimations of the nonlinearity for $x = 0.4$ by SHG with femtosecond pulses at 4.65 μm gave $d_{22}(GaS_{0.4}Se_{0.6}) = 0.76\ d_{22}(\mathrm{GaSe})$ [9]. This result, together with the large bandgap of $GaS_{0.4}Se_{0.6}$ or, in brief, GaSSe (the composition close to the maximum S content in the noncentrosymmetric structure), means that such nonlinear crystals are good candidates for application in 1064 nm pumped optical parametric oscillators (OPOs), generators (OPGs), and amplifiers (OPAs).

Two essential advantages can be expected from adding S to the well-known nonlinear crystal GaSe: increase of the bandgap value or the short wave cutoff limit [10,11] and increased hardness [12], which is one of the basic limitations of GaSe. In [9], we estimated a bandgap of 2.278 eV (545 nm) for GaSSe and a useful transparency range at the 3 cm^{-1} absorption level of 0.57–14.2 μm. These parameters are 1.972 eV (629 nm) and 0.64 to 18 μm, respectively, for GaSe. In accordance with the larger bandgap, the damage threshold for GaSSe, both for nanosecond pulses and cw radiation, was roughly 50% higher than for pure GaSe [9]. Furthermore, in [13], we refined the Sellmeier equations for GaSSe based on phase-matched SHG data, showed that its two-photon-absorption (TPA) coefficient at 1064 nm is 3.5 times lower than in GaSe, and its microhardness is increased by 30% relative to GaSe. Unfortunately, the problems related to cutting, polishing, and coating of such crystals are still to be solved, and application in OPOs depends on the stability and damage resistivity of antireflection (AR) coatings. However, in OPAs pumped by high-energy ultrashort pulses, cleaved uncoated crystals can be employed and, in this work, we present such results with GaSSe using a pump system operating at 1.064 μm. This is the first real application of GaSSe in nonlinear optics, to our knowledge, and we compare the results with pure GaSe under identical experimental conditions. GaSe has been used in the past in similar schemes (pump at 1.053 μm and tunable dye laser as a seed signal) to cover the 6–18 μm idler range [14], but saturation was observed already at pump intensities beyond 0.1 GW/cm^2. Although improved results were reported later with an OPG providing the seed signal [15], as we demonstrate here, the use of GaSe is ultimately limited by TPA when pumped near 1 μm, which is not the case with GaSSe. Note that, in the low pump limit (0.1 GW/cm^2), GaSe was successfully employed and yielded sufficient parametric gain even with unamplified picosecond pump pulses [16].

As a pump source for the present OPA, we employed a mode-locked Nd:YAG laser–amplifier system at 1.064 μm with a pulse duration of 58 ps (FWHM) at a repetition rate

of 10 Hz. The seed source was derived from another OPA pumped by the second-harmonic (SH) beam from the same system at 0.532 μm (horizontal polarization), consisting of a 6-mm-long β-BaB_2O_4 (BBO) and 5-mm-long BiB_3O_6 (BIBO) crystals used in tandem for Type I (ooe) and Type II (oeo) interactions, respectively. In this OPA system, used in a double-pass configuration, the BBO serves as an OPG in the first pass and as a broadband amplifier in the second pass, which is seeded by the narrow signal spectrum from Type II OPA in BIBO with an appropriate pump delay realized by translation of the M3 mirror in Fig. 1.The vertically polarized idler beam from the OPA system, with energy in the 1–10 μJ range, depending on the wavelength, which could be varied between 1.175 and 1.4 μm, is then collinearly mixed in GaSSe or GaSe with the collimated fundamental beam at 1.064 μm (horizontal polarization) through the bending mirror M5. In the present OPA experiment, the Type II (eoe) process is chosen rather than the Type 1 (ooe) process, considering the fact that it provides higher idler output in the absence of an AR coating because of the much lower surface reflection for p polarization (this was confirmed by comparing the idler output for both processes under the same experimental conditions).

Figure 2(a) shows the idler energy measured at a wavelength of 6.45 μm versus pump intensity at 1.064 μm at fixed SH energy of 1.6 mJ (after the bending mirror M1) for pumping the BBO–BIBO seeder. At the actual phase-matching angles, effective nonlinearities of 38 and 49 pm/V are estimated for GaSSe and GaSe, respectively. Taking into account the ~20% lower figure of merit of GaSSe, a 4.7-mm-long c-cut sample was prepared for fair comparison with a 3.9-mm-long GaSe sample. For the beam diameters and pulse durations in the present experiment, spatial and temporal walk-off effects can be neglected. At low pump intensity (<0.2 GW/cm^2), the idler energies with GaSSe and GaSe were very similar, as expected from the calculated parametric gain factors. However, when the pump intensity was further increased, GaSSe showed superior performance. At a pump intensity of 1.08 GW/cm^2 (~2.8 mJ incident pump energy at 1.064 μm), the idler energy reached 9.1 μJ, about 3 times higher than with GaSe. The behavior of GaSe was similar to that observed in [14]; however, we attribute the "saturation" not to pump depletion but to nonlinear pump losses, e.g., TPA at 1.064 μm, as confirmed experimentally.

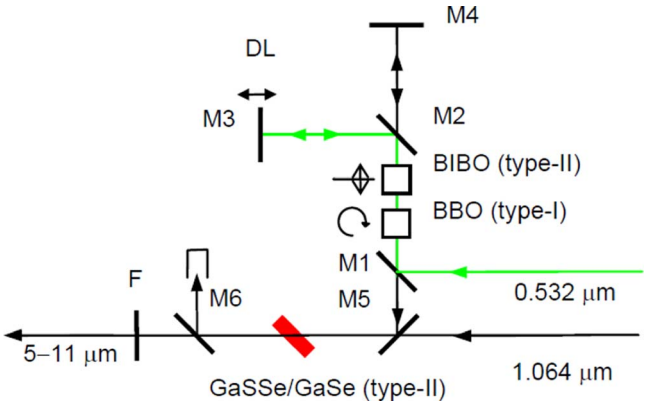

Fig. 1. (Color online) Schematic of the experimental setup for OPA in GaSSe and GaSe. M1–M3, 0.532 μm highly reflective (HR) dichroic mirrors; M4, metallic mirror; M5, 1.15–1.4 μm HR dichroic mirror; M6, 1.064 μm HR dichroic ZnSe mirror; F, 2.5 μm cut-on filter; DL, delay line.

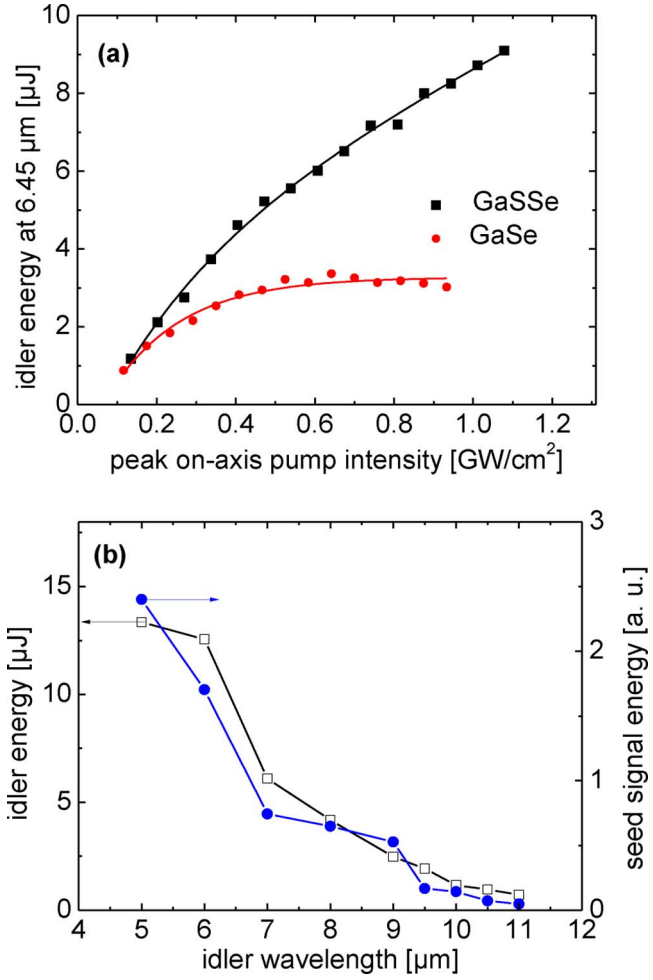

Fig. 2. (Color online) (a) Idler energy at 6.45 μm versus pump intensity of the GaSSe and GaSe OPAs and (b) idler tuning achieved with GaSSe at maximum pump level. The peak on-axis pump intensity inside the crystal is calculated by using the actual value of the pump pulse duration of 76 ps (as a result of SH depletion), the beam size inside the crystal, and by correcting by the Fresnel reflection at the input surface.

The tuning performance of GaSSe (5–11 μm) is determined in the present experiment to a great extent by the available seed energy at the signal wavelength [Fig. 2(b)]. The pulse duration was estimated from autocorrelation measurements using noncollinear SHG in an ~3-mm-thick Type I GaSe crystal. The estimated idler pulse FWHM (fitting with Gaussian pulse shapes) was 26 ps at 4.8 μm and 29 ps at 6.45 μm [Figs. 3(a) and 3(b)], shorter than the pump pulse duration, as could be expected.

Since our TPA studies in [13] were confined to the o-polarization (c-cut crystals used at normal incidence), we remeasured the nonlinear losses for the samples used in the present experiment with the p-polarized pump at 1064 nm, which represents a mixed polarization (e and o) at the actual OPA phase-matching angle. The linear losses, which were independently determined using a cw Nd:YVO_4 laser, were substantially higher (absorption coefficient $\alpha \sim 0.29\ \mathrm{cm}^{-1}$) in GaSe as compared to GaSSe

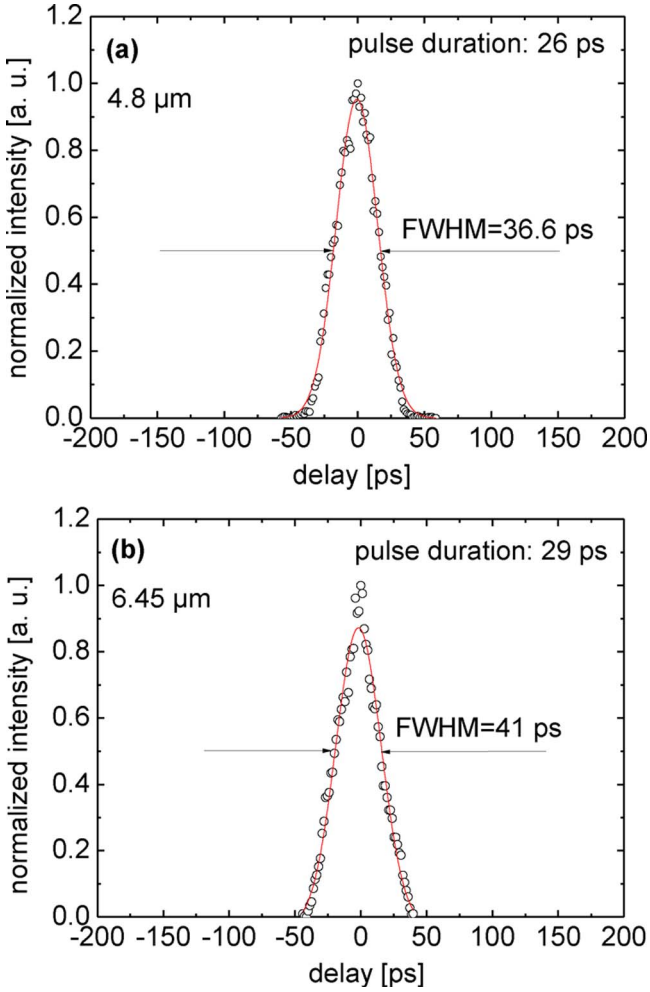

Fig. 3. (Color online) Autocorrelation functions recorded for the GaSSe OPA at idler wavelengths of (a) 4.8 and (b) 6.45 μm.

($\alpha \sim 0.07\,\mathrm{cm}^{-1}$). At a peak on-axis pump intensity of $1\,\mathrm{GW/cm}^2$ inside the crystal, the TPA coefficient estimated for GaSe was $\beta \sim 4\,\mathrm{cm/GW} \pm 15\%$, roughly 1 order of magnitude higher than the corresponding value estimated for GaSSe. Thus, the superior performance of the GaSSe OPA in Fig. 2(a) is attributed to the suppressed TPA effect at the pump wavelength due to its larger bandgap.

In conclusion, we demonstrated that the mixed GaSSe crystal can be used for downconversion to the mid-IR with powerful $\sim 1\,\mu$m pump sources. In comparison to the few other nonlinear chalcogenide crystals that exhibit no TPA at this wavelength (e.g., $AgGaS_2$), GaSSe possesses the best potential to cover deep mid-IR wavelengths, reaching $\sim 14\,\mu$m.

The research leading to these results has received funding from the European Community's Seventh Framework Programme FP7/2007-2011 under grant agreement n°224042.

References

1. K. R. Allakhverdiev, R. I. Guliev, E. Yu. Salaev, and V. V. Smirnov, Sov. J. Quantum Electron. **12**, 947 (1982), translated from Kvantovaya Elektron. (Moscow) **9**, 1483 (1982).
2. H. Serizawa, Y. Sasaki, and Y. Nishina, J. Phys. Soc. Jpn. **48**, 490 (1980).
3. C. H. Ho, C. C. Wu, and Z. H. Cheng, J. Cryst. Growth **279**, 321 (2005).
4. K. R. Allakhverdiev, M. Ö. Yetis, S. Özbek, T. K. Baykara, and E. Yu. Salaev, Laser Phys. **19**, 1092 (2009).
5. G. B. Abdullaev, K. R. Allakhverdiev, R. Kh. Nani, E. Yu. Salaev, and M. M. Tagyev, Phys. Status Solidi A **53**, 549 (1979).
6. C. Perez Leon, L. Kador, K. R. Allakhverdiev, T. Baykara, and A. A. Kaya, J. Appl. Phys. **98**, 103103 (2005).
7. S. Das, C. Ghosh, O. G. Voevodina, Yu. M. Andreev, and S. Yu. Sarkisov, Appl. Phys. B **82**, 43 (2006).
8. H.-Z. Zhang, Z.-H. Kang, Y. Jiang, J.-Y. Gao, F.-G. Wu, Z.-S. Feng, Y. M. Andreev, G. V. Lanskii, A. N. Morozov, E. I. Sachkova, and S. Yu. Sarkisov, Opt. Express **16**, 9951 (2008).
9. V. Petrov, V. L. Panyutin, A. Tyazhev, G. Marchev, A. I. Zagumennyi, F. Rotermund, F. Noack, K. Miyata, L. D. Iskhakova, and A. F. Zerrouk, Laser Phys. **21**, 774 (2011).
10. G. A. Akhundov, N. A. Gasanova, and M. A. Nizametdinova, Phys. Status Solidi B **15**, K109 (1966).
11. C. C. Wu, C. H. Ho, W. T. Shen, Z. H. Cheng, Y. S. Huang, and K. K. Tiong, Mater. Chem. Phys. **88**, 313 (2004).
12. P. G. Rustamov, Z. D. Melikova, M. G. Safarov, and M. A. Alidzhanov, Inorg. Mater. **1**, 387 (1965), translated from Izv. Akad. Nauk. SSSR, Neorganicheskie Materialy **1**, 419 (1965).
13. G. Marchev, A. Tyazhev, V. Panyutin, V. Petrov, F. Noack, K. Miyata, and M. Griepentrog, Proc. SPIE **7917**, 79171G (2011).
14. T. Dahinten, U. Plödereder, A. Seilmeier, K. L. Vodopyanov, K. R. Allakhverdiev, and Z. A. Ibragimov, IEEE J. Quantum Electron. **29**, 2245 (1993).
15. I. M. Bayanov, R. Danielius, P. Heinz, and A. Seilmeier, Opt. Commun. **113**, 99 (1994).
16. G. I. Petrov, K. L. Vodopyanov, and V. V. Yakovlev, Opt. Lett. **32**, 515 (2007).